 DOI: 10.1002/masy.200950801

Molecular Weight and Branching Distribution of a High Performance Metallocene Ethylene 1-Hexene Copolymer Film-Grade Resin

M. Vadlamudi,[1] *G. Subramanian,*[1] *S. Shanbhag,*[1] *R. G. Alamo,**[1] *M. Varma-Nair,*[2] *D. M. Fiscus,*[3] *G. M. Brown,*[3] *C. Lu,*[3] *C. J. Ruff*[3]

Summary: The bivariate, or cross branching distribution of a gas-phase produced, film-grade ethylene 1-hexene copolymer with enhanced Elmendorf tear in machine direction, MD, and in transverse direction, TD, ($>$ 400 g/mil) and high dart impact has been characterized through the analysis of fractions obtained by molecular weight and 1-hexene composition. The molecular weight fractions, obtained by a solvent-non-solvent fractionation technique, are each mixtures of molecules with at least two different 1-hexene compositions, one component with a constant relatively high density ($\sim$1 mol% hexene) and a second of a lower density broadly distributed along the molecular weight fractions. The content of the low density component increases with increasing molecular weight of the fraction while the level of 1-hexene decreases. The mixed compositional character of these fractions is easily inferred by their high crystallization rates and both high melting and crystallization temperatures compared to the values of model random ethylene copolymers. The set of compositional fractions obtained by TREF display an increasing 1-hexene concentration with increasing molecular weight, and except for the highest molecular weight components (Mw $>$ 150,000 g/mol) their melting and crystallization behavior followed the random pattern. Higher than expected melting temperatures and a constancy of the high melting temperature peak with increasing crystallization temperature, suggests that the intra-chain 1-hexene distribution of the highly branched, high molecular weight fraction deviates strongly from the random behavior. These structural features and the bimodal character of the composition distribution of this resin, that contains high molecular weight chains with both low and high 1-hexene contents, are correlated with the enhanced key film properties.

Keywords: bimodal branching distribution; ethylene 1-hexene; ethylene copolymers; gas-phase LLDPE

Introduction

A rich variety of combinatorial catalysts and advances in organometallic chemistry and in coordination catalysis has provided the polyolefin industry with the means to engineer novel products and the possibility to tailor molecular microstructures with unique performance. The advent of metallocene chemistry has played a major role in laying out this path.[1,2] These catalysts provide excellent control of stereoregularity and copolymerization with polar and other types of comonomers that was not possible with the classical Ziegler-Natta catalyst systems. The single site nature of

[1] FAMU/FSU College of Engineering, Department of Chemical Engineering 2525 Pottsdamer St., Tallahassee, FL 32310, USA
E-mail: alamo@eng.fsu.edu
[2] ExxonMobil Research and Engineering Co., Rt 22 East, Annandale, NJ 08801, USA
[3] ExxonMobil Chemical Co., 5200 Bayway Drive, Baytown, TX 77522, USA

the metallocene catalyst leads to LLDPEs with narrow molecular weight and narrow inter-chain comonomer composition. An early benefit of the metallocene chemistry was the production of polyethylene resins with bimodal molecular weight distributions and a preferred introduction of the comonomer in the longest chains for a superior process/properties balance.[3,4] This microstructure differs from the characteristic inter-chain comonomer distribution given by classical Ziegler-Natta catalysts where the shorter chains have the highest concentration of comonomer.[5] It has been speculated that the incorporation of the comonomer in the high molar mass portion of the distribution increases the number of tie-chains (molecules that connect two or more crystallites) accounting for better balanced properties and enhanced impact.[6]

Although this concept was initially engineered via blending different proportions of high and low molecular weight metallocene LLDPEs with high or low comonomer contents,[7] resins with bimodal comonomer composition distribution (BCD) and/or bimodal molecular weight distribution were subsequently synthesized using tandem (staggered) series reactors. Special attention was given to properties of LLDPEs with a placement of the comonomer as a function of molecular weight reversed or orthogonal to the standard distribution of Z/N catalyzed LLDPEs, i.e., with an increasing comonomer content with increasing molecular weight. These resins are referred as having bimodal orthogonal comonomer composition distribution (BOCD). The process and properties of LLDPE resins of this type made in single gas-phase reactors are described in a US 2005 patent.[8] A film grade ethylene 1-hexene resin (1.0 MI, 0.920 g/cm^3 density) produced following this method resulted in enhanced Elmendorf tear in the machine and transverse directions, MD and TD (>400 g/mil), over the present resins values,[4] and with high dart impact. Our interest here is to characterize the details of the distribution of the content of 1-hexene across the molecular weight distribution of this novel resin. This is accomplished by characterizing the branching and chain length microstructure of two sets of fractions, one set was obtained by molecular weight fractionation using a standard solvent/non-solvent technique, and a second set fractionating by the 1-hexene content via preparative TREF. The availability of independent fractions allows comparative analysis of the bivariate distribution profiles obtained from each type of fractionation. In addition, the thermal properties and crystallization behavior of both types of fractions are discussed in reference to the behavior of random model ethylene copolymers and single site metallocene-made LLDPEs that are known to have a nearly equivalent inter-chain comonomer content and random intra-chain distribution.

Experimental Part

The starting metallocene catalyzed 1-hexene LLDPE resin was recently produced in a commercial gas-phase Unipol-type reactor using standard conditions and the methodology described in reference 8. The whole resin was fractionated by molecular mass into 10 fractions using the solvent/non-solvent fractionation technique (these fractions are termed M fractions).[9] The fractionation was carried out at 130 °C using xylene/diethylene glycol monobutyl ether (DEGME) as solvent/non-solvent pair. The content of non-solvent was varied between 60 and 41%. Both solvents were stabilized with 600 ppm of BHT (butylated hydroxy toluene). A set of 11 comonomer composition fractions was also obtained using preparative temperature rising elution fractionation (TREF) in a CRYSTAF-TREF instrument, Model MC2 manufactured by Polymer Char S.A., Valencia, Spain, with ortho-dichloro benzene (o-DCB) as elution solvent, stabilized with 300 ppm of BHT (T fractions).[10,11] The 0.4 g/100cc solution was dissolved at 160 °C, subsequently

stabilized at 95 °C, and slowly cooled from 95 °C to −20 °C at a rate of 0.5 °C /min. In a second step TREF fractions were collected raising the temperature in a range from -20 to 120 °C. Data for molecular characterization of the fractions are listed in Table 1.

The average molecular weights of the whole polymer and both sets of fractions were determined by standard Gel Permeation Chromatography (GPC) and the average comonomer composition was obtained using solution ^{1}H NMR. TREF profiles of each individual M or T fraction were also collected. Crystallizations and further melting were followed by DSC at 10 °C/min using a Perkin Elmer DSC-7 calibrated with indium and operating under nitrogen flow. The sample mass was about 4 mg. The DSC was calibrated for static temperature and thermal lag effects with indium. Overall isothermal crystallization rates were associated with the inverse of the time corresponding to the exothermic DSC peak. The DSC was connected to an intracooler to maximize heat transfer and allow sub-ambient temperature control. The crystalline morphology was analyzed by optical microscopy (OM), small angle light scattering (SALS) and thin section transmission electron microscopy (TEM) after staining with RuO_4.

Results and Discussion

Fractionation

All M fractions, obtained by solvent/non-solvent fractionation, have narrow molecular weight distribution ($Mw/Mn \leq 1.7$) and display a systematic increase of Mn and Mw along the fractionation process (i.e., increasing xylene content). Compared to the broad GPC profile of the unfractionated resin, the GPC profiles of each M fraction are unimodal and relatively narrow, as depicted in Figure 1(a).

The average content of butyl branches of M fractions (determined by NMR) changes slightly in a narrow range, between 1 and 2 mol% (branches per 100 backbone carbons). However, the TREF profiles of each M fraction are bi or tri-modal, as shown in Figure 1(b), indicating that the branching content determined by NMR spectroscopy is an average of at least two branching compositions. TREF profiles are analyzed on the basis of compositional partitioning during crystallization.[12] This analysis assumes that molecules of low comonomer content do not co-crystallize with molecules having a higher comonomer content, consequently, the crystallites formed from the former will dissolve (elute) at higher temperatures. The two-three peaks

Table 1.
Molecular weight and NMR branching data of the whole ethylene 1-hexene initial resin and fractions. M-F# refers to molecular weight fractions and T-F# refers to TREF fractions.

Molecular Weight Fractions						Comonomer Composition Fractions					
Fraction ID	% DEGME	Mn x 10^{-3} (g/mol)	Mw x 10^{-3} (g/mol)	Mw / Mn	Branch points (mol%)	Fraction ID	Collection Temperature Range (°C)	Mn x 10^{-3} (g/mol)	Mw x 10^{-3} (g/mol)	Mw / Mn	Branch points (mol%)
Parent resin		34	123	3.6	1.66	Parent resin	–	34	123	3.6	1.66
M-F1	60.0	5.8	10	1.7	1.42	T-F1	< 15	15	231	15.4	5.48
M-F2	53.0	13	18	1.4	0.89	T-F2	15 to 36	44	249	5.7	3.53
M-F3	49.0	23	35	1.5	1.13	T-F3	36 to 51	19	169	8.8	3.14
M-F4	47.0	33	48	1.5	1.34	T-F4	51 to 59	30	207	6.8	2.85
M-F5	44.3	51	86	1.7	1.57	T-F5	59 to 65	37	170	4.6	2.10
M-F6	43.0	68	118	1.7	1.73	T-F6	65 to 71	27	131	4.8	1.61
M-F7	42.4	92	156	1.7	1.78	T-F7	71 to 77	24	95	3.9	1.13
M-F8	41.9	112	187	1.7	1.81	T-F8	77 to 83	24	70	2.9	0.76
M-F9	41.3	147	234	1.6	1.81	T-F9	83 to 87	24	59	2.5	0.52
M-F10	0	226	336	1.5	1.74	T-F10	87 to 91	26	57	2.2	0.44
						T-F11	>91	31	61	1.9	0.46

The percentage of non-solvent (DEGME) and temperature range for collection of molecular weight and compositional fractions respectively are also listed.

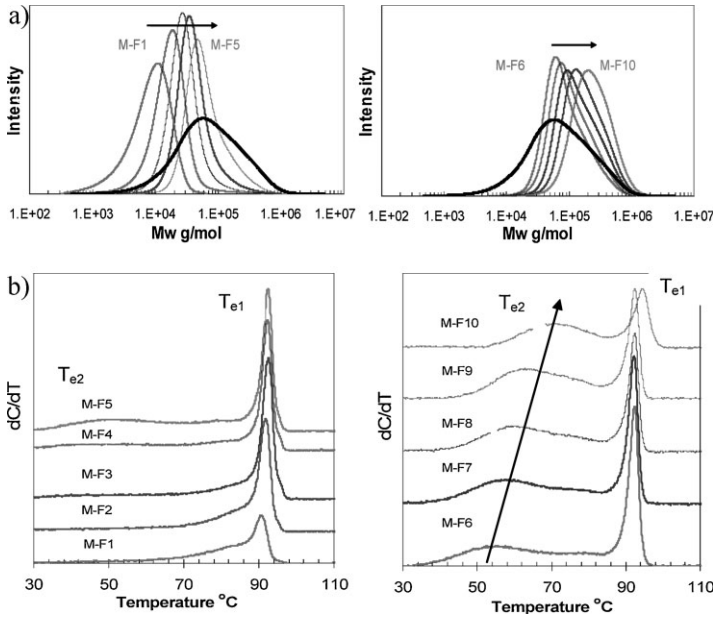

Figure 1.
(a) GPC profiles of M Fractions. The curves shift systematically to higher values with increasing fraction number. The profile of the unfractionated resin is shown as black thicker line. (b) TREF profiles of M Fractions.

observed in the TREF profiles of M fractions represent molecules of equivalent length with different 1-hexene composition. All M fractions contain a population of chains with a fixed low 1-hexene content that elute at about the same temperature, ~92 °C, labeled T_{e1} in the figure. A second population of crystals (T_{e2}) dissolves in a broad (40–80 °C) and lower range of temperatures and correspond to chains with a higher content of 1-hexene. The value of T_{e2} increases with fraction number reflecting a decreasing content of 1-hexene as the molecular weight of this population of chains increases. The intensity of T_{e2} increases with Mw and levels off for fractions beyond M-F8, indicating a progressive increase in the weight fraction of the highly branched component with increasing molar mass up to Mw ~ 190,000. A lower intensity peak at ~80 °C, also present in all fractions, may indicate a third compositional component of intermediate branching content.

Eleven (11) fractions were also collected by preparative temperature rising elution fractionation (TREF) in order to isolate chain components with different branching composition. These fractions provide direct evidence of the progressive compositional nature of chains eluting in the range of temperatures marked as T_{e2} in Figure 1(b). The average molecular masses and NMR compositional data are listed in Table 1. Fractionation by preparative TREF separates copolymer molecules preferentially by comonomer content.[10–12] Molecules with the highest 1-hexene content lead to thin crystallites that dissolve (elute) at the lowest temperatures, providing not co-crystallization occurs with chains having a lower 1-hexene content. Co-crystallization, although not totally avoided, is minimized by increasing dilution and slowing down the initial crystallization step prior to elution, for example reducing the cooling rate. Crystallites formed from molecules with the lowest 1-hexene content are the last to dissolve and elute at the highest temperatures. The expected systematic decrease of branching with increasing elution temperature is indeed observed in the data for T

fractions of Table 1 with 1-hexene content changing from 5.48 to 0.44 mol% among the fractions. The increase in branching parallels the increase in Mw, following the characteristics of BOCD resins. It does not follow a systematic increase with Mn because of the large polydispersity in chain length of fractions with a fixed content of 1-hexene, as shown by the relatively high Mw/Mn values in the Table. Details of chain length distribution and homogeneity of 1-hexene content distribution of each T fraction are extracted from the GPC and TREF profiles of each TREF fraction shown in Figure 2(a,b).

Unimodal distributions are the general features of the T fractions, except for a small peak in the low molecular weight side of the GPC profiles and between 85 and 95 °C in the TREF profiles. The GPC curves are relatively broad, as expected from the results of Figure 1b, while the TREF profiles of Figure 2b are narrow and progressively shift to higher temperatures, as the content of 1-hexene decreases. Notice that the least branched fractions, T-F10 and T-F11, are expected to have much broader molecular weights than lower T fractions (T-F1 – T-F3), as the molecules of T-F10 and T-F11 correspond to the T_{e1} component of all M fractions (see Figure 1b). One explanation for the relatively narrow GPG profiles of T-F10 and T-F11 is that some of the molecules in the 10^3–10^4 molecular weight range elute with highly branched molecules at the lowest elution temperatures. This would explain the small peaks in the profiles of

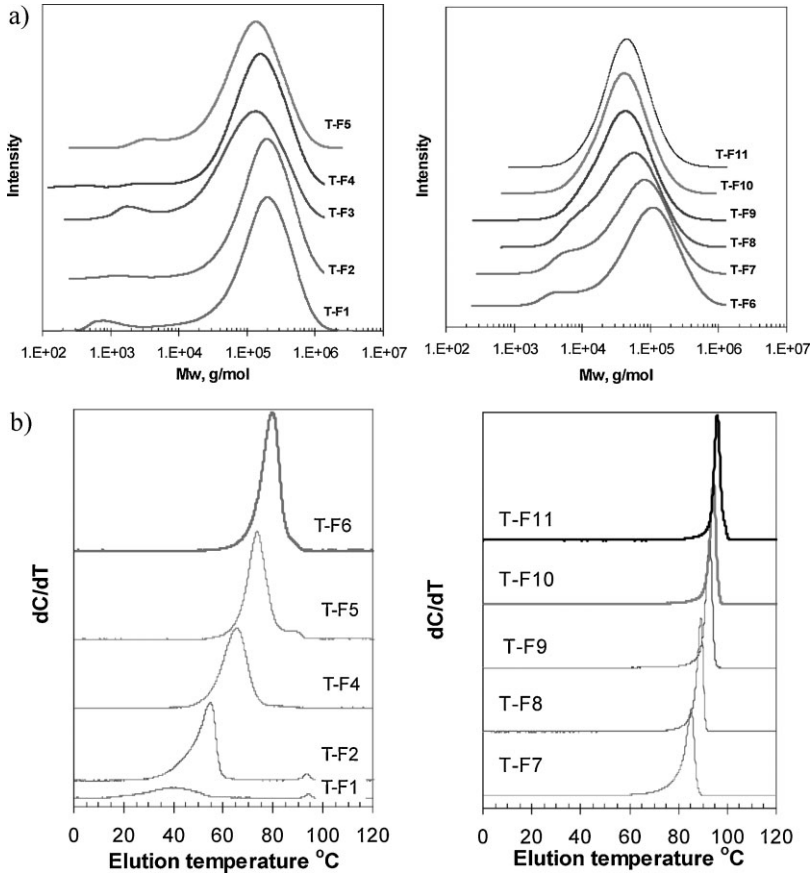

Figure 2.
(a) GPC profiles of each T fraction. (b) TREF profiles of each T fraction

Figure 2(a) and at ~93 °C in the profiles of T-F1 to T-F5 of Figure 2(b). Moreover, repeated TREF fractionations led to very similar results.

A two-dimensional plot of the average Mw data of each TREF fraction over the TREF profile of the unfractionated LLDPE, such as Figure 3, is often used to characterize the molecular weight – comonomer content cross-distribution of these copolymers.[4] In a further step, Ortin et al. in 2007 described an automated method to represent in a 3D map the molecular weight distributions of TREF eluted material in a range of temperatures.[13]

According to Figure 3, the characteristics of the cross - distribution of the novel resin appear analogous to a BOCD copolymer because the comonomer content increases with the average Mw data. However, this is not accurate since GPC and TREF profiles of M-F8 to M-F10 fractions indicate that the initial resin contains high molecular weight chains (~200,000 g/mol) with both, relatively low and high 1-hexene content, as shown in Figure 1(b).

Having characterized individually M and T fractions for their length (GPC) and comonomer (TREF elution temperatures) distributions, the joint Probability Density Functions (PDF) or bivariate distributions were computed separately for each M and T sets of fractions. The bivariate three-dimensional distribution was constructed assuming independence of the molecular weight distributions (MWD) and elution temperature distributions (ETD). From the GPC and TREF profiles of M fractions the bivariate was obtained as:

$$f_M(m,t) = \frac{\sum_{i=1}^{i=10} w_{M\text{-}Fi} f_{M\text{-}Fi}(m) f_{M\text{-}Fi}(t)}{\sum_{i=1}^{i=10} w_{M\text{-}Fi}}$$

and from the GPC and TREF profiles of T fractions as:

$$f_T(m,t) = \frac{\sum_{j=1}^{j=11} w_{T\text{-}Fj} f_{T\text{-}Fj}(m) f_{T\text{-}Fj}(t)}{\sum_{j=1}^{j=11} w_{T\text{-}Fj}}$$

Where:

$f_{M\text{-}Fi}$ (m) = Logarithmic molecular weight distribution of M fraction M-Fi

$f_{T\text{-}Fj}$ (m) = Logarithmic molecular weight distribution of TREF fraction T-Fj

$f_{M\text{-}Fi}$ (t) = TREF profile of M fraction M-Fi

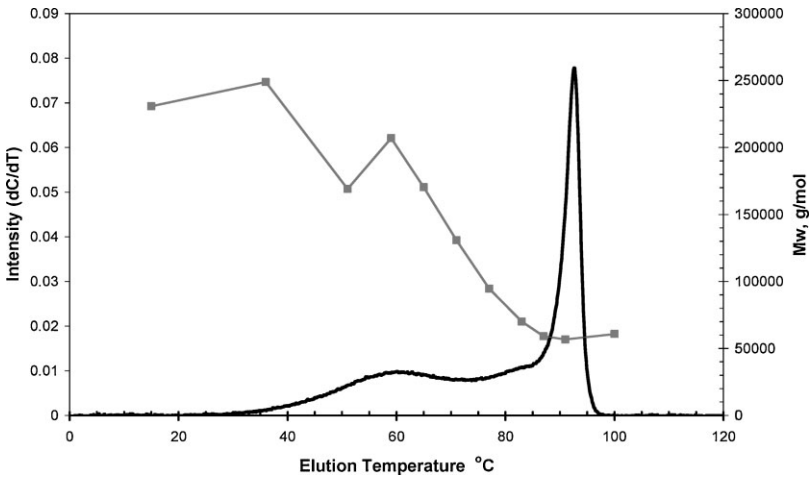

Figure 3.
TREF profile of whole resin and weight average molecular weight of TREF fractions (filled squares) collected at the indicated elution temperature.

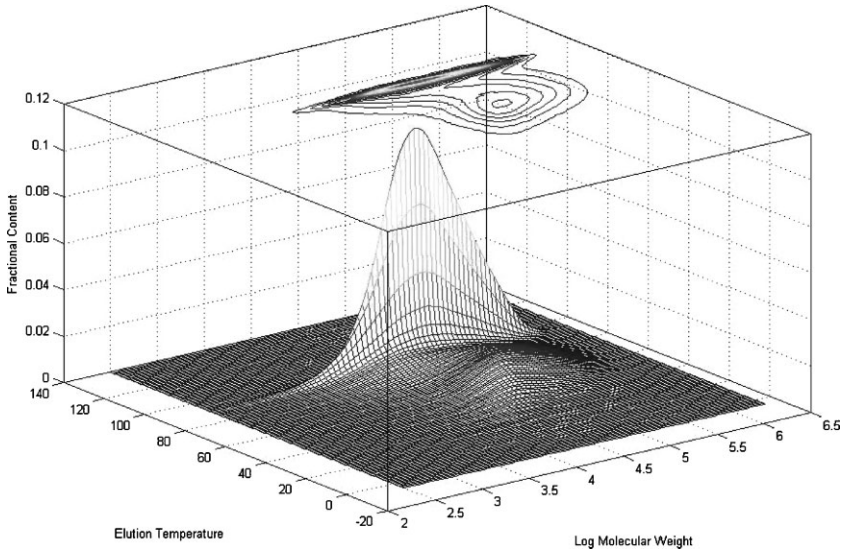

Figure 4.
Bivariate distribution and surface contour from data corresponding to M fractions.

$f_{T\text{-}Fj}$ (t) = TREF profile of TREF fraction T-Fj
$w_{M\text{-}Fi}$ = Weight fraction of M fraction M-Fi
$w_{T\text{-}Fj}$ = Weight fraction of TREF fraction T-Fj

Using spline interpolation for data smoothing, PDF distributions are plotted in Figure 4 (from data of M fractions), and in Figure 5 (from data of T fractions). Both plots display graphically the same general unique complex bimodal 1-hexene composition distribution of the resin. The heights of the 3-D profile indicate two major components moving in increasing direction of the elution temperature axis (inversely proportional to the comonomer content). One component corresponds to chains that elute in a narrow temperature range, at ~95 °C (~1 mol% 1-hexene). These molecules have narrow 1-hexene content and broad molecular weight distribution. A second component corresponds to molecules that elute in a broad temperature range, between 20 and 90 °C. The range of comonomer content of the latter molecules is broad, between 11 and 2 mol% 1-hexene, and have somewhat narrower molecular weight distribution than the range of the first component. Although there is agreement in the general features of the PDF distribution from both sets of fractions, the contour topological view or weight fraction distribution is not identical. The mismatch reflects experimental uncertainties from each type of fractionation. For example, the solvent non-solvent technique leads to fractions that are not unimodal in chain length, and the extent to which co-crystallization may occur during TREF preparative fractionation, and thus affect the TREF profiles is unknown. The uncertainties from both fractionation types are averaged in the joint PDF, f (m,t) as:

$$f(m,t) = \frac{f_M(m,t) + f_T(m,t)}{2}$$

with f_M (m, t) and f_T (m, t) given as:

f (m, t) = Joint PDF of specimens fractionated by TREF, and by molecular weight
f_M (m, t) = Joint PDF of molecular weight fractions
f_T (m, t) = Joint PDF of TREF fractions

The combined profile is shown in Figure 6.

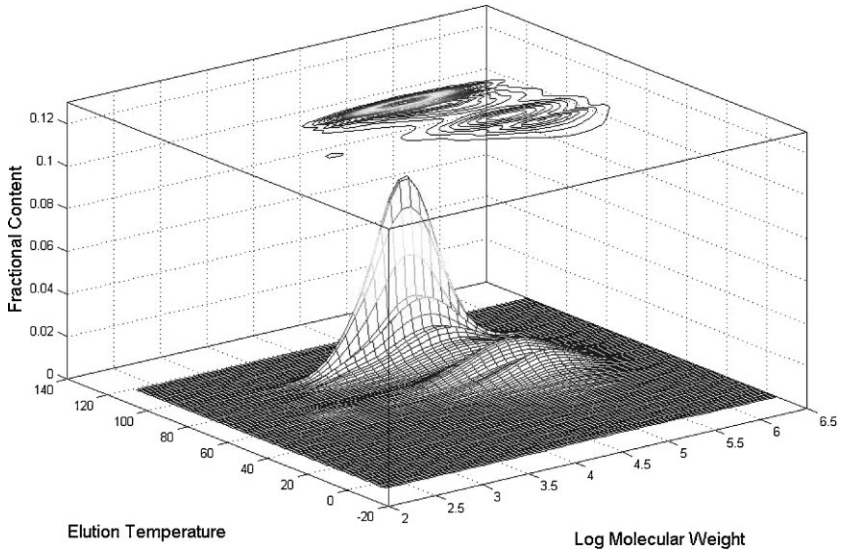

Figure 5.
Bivariate distribution and surface contour from data corresponding to T fractions.

The fractional content of the high-density component, obtained from the volume above a temperature range of 80–85 °C, corresponds to 59–52%. Conversely, medium and highly branched molecules make for 41–48% by weight of the enhanced resin.

Melting Behavior

The advantage of having molecular weight and compositional fractions physically separated, with respect to other automated modes of characterizing the bivariate distribution,[13,14] is that additional analyses can be carried out in the fractions for

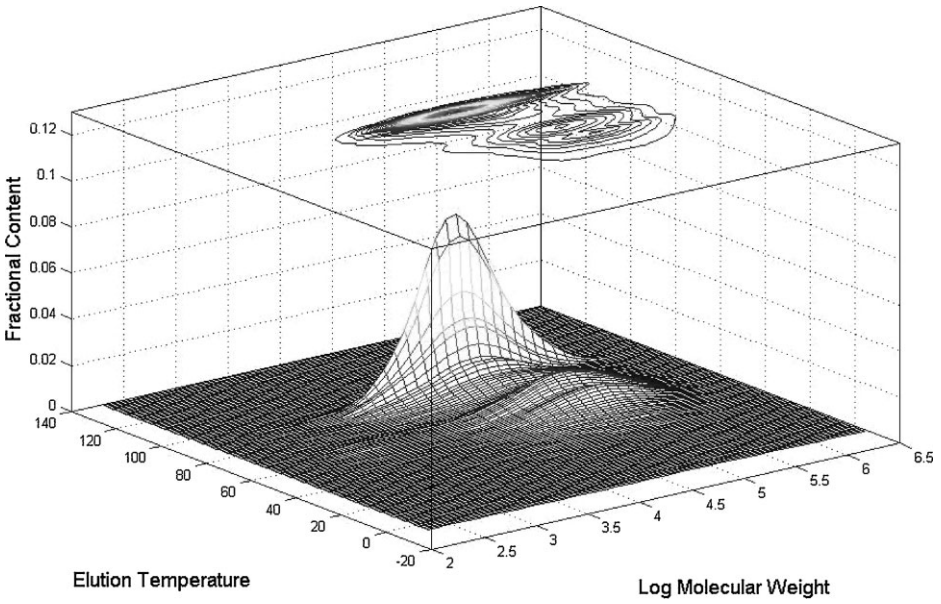

Figure 6.
Joint bivariate distribution and surface contour from data corresponding to M and T fractions.

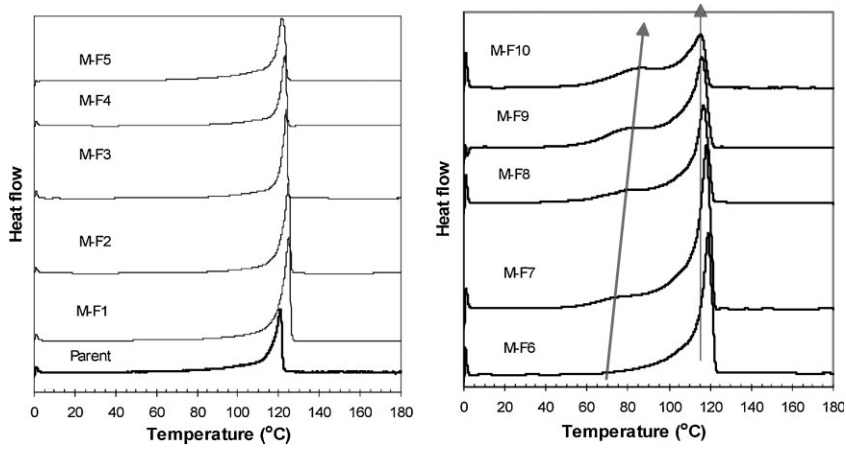

Figure 7.
Melting endotherms of molar mass fractions (M fractions) after cooling from the melt at 10 °C/min. The arrows indicate the variation of the bimodal comonomer composition with increasing molecular weight.

conformity with expectations from the PDF distribution. For example, TREF analyses of the individual M fractions indicated compositional heterogeneity of molecules with a fixed length, possibly of a bimodal nature. This feature is tested by analyzing the melting behavior of these fractions in reference to the behavior of random ethylene copolymers of matched comonomer content narrowly distributed across an also narrow molecular weight distribution. Melting data for the latter are available from previous works.[15–18]

Under relatively rapid crystallization, the melting of hydrogenated polybutadienes and narrowly distributed metallocene copolymers is single peaked, while double melting is expected for fractions with a bimodal 1-hexene content. As seen in Figure 7 most M fractions display double melting. The variation of the peak melting temperature as a function of molecular weight is given in Figure 8(a) where the continuous line represents the data of hydrogenated polybutadienes (HPBDs) with 2.2 mol% ethyl branches.[16] HPBDs are model materials analogs to random ethylene 1-butene copolymers. They have very narrow molecular weight distribution (~1.2), uniform inter-chain branching content and a random intra-chain distribution of branches. Since both, the ethyl and the

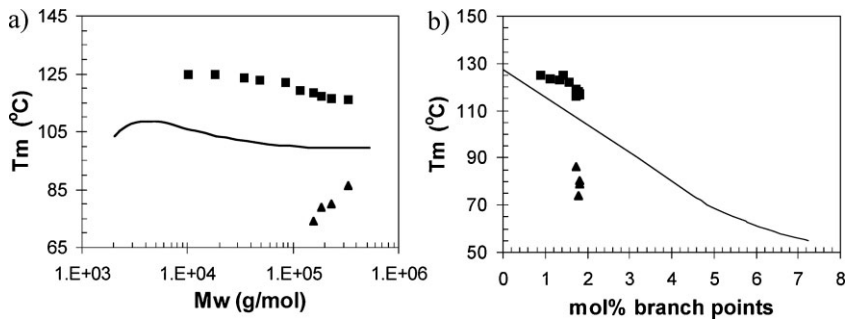

Figure 8.
Variation of the melting peak of M fractions with molecular weight (a) and with mol% of branch points (b). Squares and triangles denote bimodal melting (see text). The continuous lines represent the melting behavior of model random ethylene 1-alkene copolymers (ethyl and longer branches) extracted from references 15 – 18.

butyl branch are excluded from the crystalline regions, HPBDs are ideal copolymers to test for inter-molecular compositional heterogeneity or for the non random intra-molecular branching distribution in matched ethylene copolymers.

The observed double melting for M fractions with Mw > 100,000 g/mol is in agreement with the bimodal comonomer composition behavior inferred from the TREF profiles, earlier referred as T_{e1} and T_{e2} components. Note in Figure 8(a) the modest decrease of the highest melting peak with increasing molecular weight, paralleling the trend of the model HPBDs.[16] This reflects that all M fractions have one population of molecules with similar low 1-hexene content (lower than 2 mol%). In contrast, the low temperature peak increases over 20 degrees with increasing molecular weight, indicating molecules with higher branching content (>2 mol%), or a lower density component. The 1-hexene content of the latter decreases with increasing molecular weight, as it is inferred by the corresponding increase in melting temperature. Since the NMR determined branching content (listed on Table 1) is the average value from both compositions weighted by the relative mass of all components in each M fraction, plots of the observed melting temperatures versus the NMR averaged branching content, such as Figure 8(b), contain data that are above or below the HPBD data. Data above the reference line correspond to melting of crystallites formed from the high-density component of the M fractions, while those below the line correspond to the lower density component of the same fraction.

As shown, the melting behavior gives additional evidence for the heterogeneous compositional nature of the molecular weight fractions. Each fraction is a mixture of chains with two different l-hexene contents. This heterogeneity also affects the DSC-measured isothermal crystallization rates of M fractions which are led by the lowest l-hexene component and are significantly higher than those of HPBDs at matched branching content.

The compositional heterogeneity of M fractions leads to lamellar morphologies that clearly differ from those of homogenous matched copolymers, as found in the representative TEM images given in Figure 9. Here the morphology of M-F9 is compared with a compositionally matched narrow metallocene under the same slow crystallization. The bimodal lamellar size distribution seen in M-F9 (left micrograph)

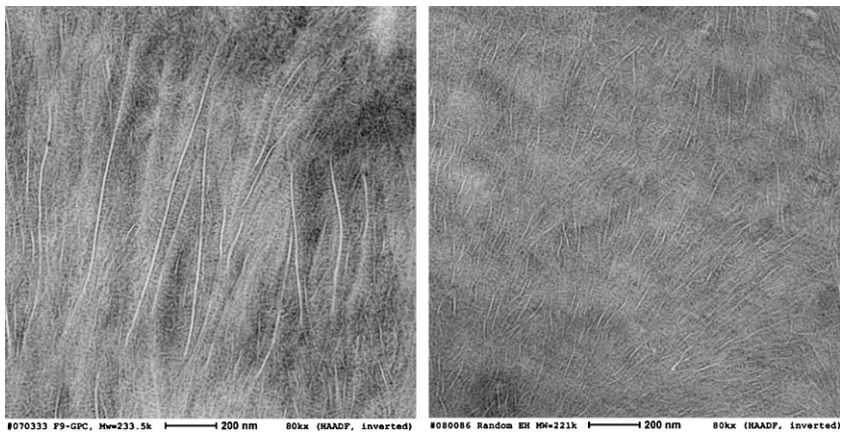

Figure 9.
TEM micrographs of M-F9 (1.81 mol% branches, Mw = 234,000 g/mol) (left), and narrow metallocene ethylene 1-hexene (2.2 mol% branches, Mw = 221,000 g/mol, Mw/Mn = 2.1) (right). Specimens were slowly crystallized from the melt at 1 °C/min.

contrasts with a more homogeneous lamellar distribution observed at the same magnification for a narrow metallocene ethylene l-hexene copolymer of similar mol % branching. The high-density component or lowly branched molecules of M-F9 develop long crystalline lamellae, with thicknesses of ~112 Å and spanning lengths over 1.5 μm, while molecules of M-F9 with higher branching content form much shorter lamellae with thicknesses of ~70 Å. In the random ethylene 1-hexene copolymer, the long thick lamellae are absent because the comonomer composition is uniform, thus the average crystallizable ethylene sequence length is shorter than the value corresponding to the lowly branched component in the M-F9 fraction. Correspondingly, more uniformly arranged, shorter and thinner lamella (~90 Å) are observed for the narrow copolymer.

The melting temperatures of TREF fractions are shown vs. mol % of branches in Figure 10. The continuous line is the same as in Figure 8(b), and gives the behavior of narrow random copolymers extracted from references 14 and 15. When the comonomer does not participate in the crystal, such as 1-butene and longer linear 1-alkenes, the variation of the melting temperatures of ethylene copolymers with increasing branching content is analyzed on the basis of Flory's phase equilibrium theory.[19] According to this theory, in reference to the value of the pure chain, the depression of the equilibrium melting temperature of the copolymer is independent of the type of comonomer. It only depends on the crystalline sequence propagation probability (p). For random copolymers the value of p equals the fraction of ethylene crystalline component. The melting of compositional TREF fractions is analyzed on this basis to infer the random intra-molecular distribution. This is clearly an advantage of preparative TREF over automated techniques, since each fraction can be independently analyzed.

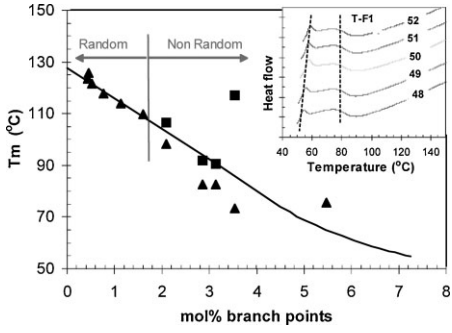

Figure 10.
Peak melting temperatures versus mol% branching of compositional fractions (T-Fractions). Square and triangles represent higher and lower melting peaks. The continuous line represents the melting behavior of model random ethylene 1-alkene copolymers (ethyl and longer branches). The inset displays DSC melting thermograms of fraction T-F1 after isothermal crystallization at the indicated crystallization temperatures (Tc).

T-fractions with < ~2 mol % branching follow the random pattern, their melting behavior is identical to the HPBDs melting. T-fractions with a higher branching display broader or double melting and deviate from the observed continuous line of the random model copolymers. This suggests an intra-chain distribution of branching that deviates from the random pattern, i.e. the chains rich in l-hexene posses a more blocky branching distribution, also supported by isothermal crystallization studies. Isothermally crystallized fractions with a low branching content melt at progressively increasing temperatures with increasing Tc as expected for random copolymers. However, as shown in the inset of Figure 10, after isothermal crystallization, the fractions with the highest l-hexene content (T–F1) have a basically constant melting, characteristic of a blocky branching distribution.

To test the possibility that higher melting crystallites are formed from lightly branched low molecular weight chains that appeared to have been flushed from the TREF column together with higher molar mass chains, a detailed solvent non-solvent fractionation was carried out on combined F-T1 to F-T2 fractions. However, very low

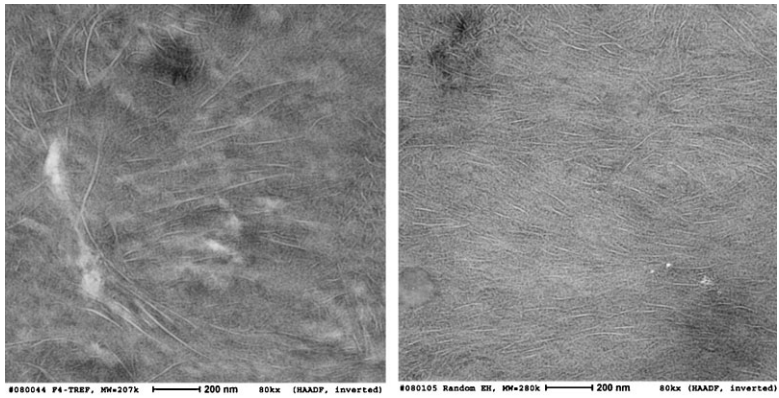

Figure 11.
TEM micrographs of T-F4 (2.85 mol% branches, Mw = 207,000 g/mol) (left) and narrow metallocene ethylene 1-hexene (3.0 mol% branches, Mw = 280,000 g/mol, Mw/Mn = 2.1), (right). Specimens were slowly crystallized from the melt at 1 °C/min.

molar mass chains could not be separated from longer ones, the three fractions obtained had double melting characteristics similar to that of the original F-T1 and F-T2. Therefore, we conclude that long crystalline sequences responsible for the higher melting appear to be an integral part of the long molecules. To further investigate the intra-molecular branching distribution of T fractions, a comonomer triad distribution analysis from ^{13}C NMR spectra is currently under study.

The lamellar morphology of T fractions in the non-random range presents features in agreement with a more blocky branching distribution. A representative example is given by the TEM micrographs of T-F4 (2.85 mol%, Mw = 207,000 g/mol, left image) and a narrowly distributed metallocene ethylene 1-hexene copolymer (3.0 mol%, Mw = 280,000 g/mol) shown in Figure 11. A more blocky distribution of comonomer in T-F4 is deduced from the fewer and longer radially oriented lamellae as compared with segmented, thinner, and more abundant lamellae of the random narrow copolymer.

Conclusion

The analysis of two sets of fractions obtained by molecular weight and comonomer composition of an ethylene 1-hexene film-grade resin with enhanced mechanical performance over classical BOCD resins, allows comparative details of the bivariate distribution obtained from each set. Both distributions display the same overall features. Gas-phase produced resins with balanced mechanical properties and Elmendorf MD tear > 400 g/mil, have a unique and complex bimodal distribution of 1-hexene over the distribution of chain lengths. The copolymer displays two major components with respect to 1-hexene content. About 50% by mass are molecules broadly distributed in chain length with a low content of 1-hexene (~1 mol%). The second component are molecules with a broad range of 1-hexene content (1.5–11 mol%) and somewhat narrower molecular weight distribution than the range of the first component. This bimodal comonomer composition of equal length chains is responsible for the observed double melting of M fractions. The high temperature melting, between 125 and 115 °C, corresponds to the lowly branched first component, while the increase of the lower melting peak from ~ 65 to 85 °C with molecular weight reflects a progressive decrease of branching content.

In addition, the melting behavior and crystalline morphology of each fraction, compared with data of model random

systems of matched composition, are useful to infer the intramolecular branching distribution. The data of Figure 10 indicate that the chains from the first component (low l-hexene content) are randomly distributed, while those forming the second component, especially highly branched molecules eluting in the 15–60 °C temperature range, have a more blocky-type l-hexene distribution. It is likely that the broad molecular weight distribution and a continuous change of l-hexene content across the molecular weight of the second component, provides for the molten chains and during crystallization an intimate mixing of high and low molecular weight components. The latter appears to be a significant factor to improve film performance.[4] Enhanced mechanical properties of this novel resin are associated with this intimate mixing.

A recent work on binary blends of linear PE and ethylene copolymers states the need to have high contents of 1-hexene preferentially incorporated in the high molecular weight chains in order to increase the concentration of tie-chains, which are responsible for superior mechanical properties of LLDPE films.[6] The branching distribution of the new ethylene 1-hexene resin points out that balanced properties and enhanced MD tear are obtained when the resin contains high molecular weight chains with both, high and low 1-hexene contents. Both components must be contributing to the connectivity between crystallites via tie-molecules. This chain connectivity reinforce properties associated with topological details of the intercrystalline region.

Acknowledgements: We are indebted to Exxon-Mobil for financial support and clearance for publication of this work.

[1] H. H. Brintzinger, D. Fischer, R. Mülhaupt, B. Rieger, R. M. Waymouth, *Angew. Chem. Int. Ed. Engl.* **1995**, *34*, 1143.
[2] P. S. Chum, K. W. Swogger, *Progress in Polym. Sci.* **2008**, *33*, 797.
[3] L. Hubert, L. David, R. Seguela, G. Vigier, C. Degoulet, Y. Germain, *Polymer* **2001**, *42*, 8425.
[4] H.-T. Liu, C. R. Davey, P. P. Shirodkar, *Macromol, Symp.* **2003**, *195*, 309.
[5] S. Anantawaraskul,1 J. B. P. Soares, P. M. Wood-Adams, *Adv. Polym. Sci.* **2005**, *182*, 1.
[6] R. K. Krishnaswamy, Q. Yang, L. Fernandez-Ballester, J. A. Kornfield, *Macromolecules* **2008**, *41*, 1693.
[7] F. C. Stehling, C. S. Speed, C. H. Welborn, *US Patent* 5, 382, 630, **1995**.
[8] J. McL Farley, J. F. Szul, M. G. McKee, *US Patent* 6 956, 088, **2005**.
[9] W. Holtrup Die, *Makromol. Chem.* **1977**, *178*, 2335–2349.
[10] L. Wild, T. R. Ryle, D. C. Knobeloch, I. R. Peat, *J. Polym. Sci., Poly. Phys. Ed.*, **1982**, *20*, 441; L. Wild, *Adv. Polym. Sci.* **1990**, *98*, 1.
[11] J. B. P. Soares, B. Monrabal, J. Nieto, J. Blanco, *Macromol Chem. Phys.* **1998**, *199*, 1917.
[12] S. Anantawaraskul, J. B. P. Soares, P. M. Wood-Adams, *Adv Polym Sci* **2005**, *182*, 1–54.
[13] A. Ortin, B. Monrabal, J. Sancho-Tello, *Macromol, Symp.* **2007**, *257*, 13–28.
[14] S. Nakano, Y. Goto, *J. Appl. Polym. Sci.* **1981**, *26*, 4217.
[15] R. G. Alamo, L. Mandelkern, *Thermochimica Acta*, **1994**, *238*, 155.
[16] R. G. Alamo, E. K. M. Chan, L. Mandelkern, I. G. Voigt-Martin, *Macromolecules*, **1992**, *25*, 6381.
[17] R. G. Alamo, L. Mandelkern, *Macromolecules*, **1989**, *22*, 1273; *idem* **1991**, *24*, 6480.
[18] R. G. Alamo, R. C. Domszy, L. Mandelkern, *J. Phys. Chem.* **1984**, *88*, 6587.
[19] P. Flory, *Trans. Faraday Soc.* **1955**, *51*, 848.

